Integrated Computer-Aided Engineering 12 (2005) 1–13 1
IOS Press

A framework for guaranteeing detection performance of a sensor network

K. Madhava Krishna[a] and Henry Hexmoor[b,*]
[a]*International Institute of Information Technology, Hyderabad – 500 019, India*
E-mail: mkrishna@iiit.ac.in
[b]*CSCE Department University of Arkansas, Fayetteville, AR 72701, USA*
Tel.: +1 479 575 2420; Fax: +1 479 575 5339; E-mail: hexmoor@uark.edu

Abstract. We present a framework for modeling and analysis for a surveillance network consisting of multiple sensors. Sensors monitor targets that crisscross a rectangular surveillance zone. When a sensor pursuits a target it leaves areas unguarded through which other targets can get past undetected. A methodology that computes the tracking time for a sensor such that a fraction of the targets expected to cross its home area is detected to an arbitrary probabilistic guarantee is presented based on the framework. Targets enter the surveillance zone according to Poisson statistics. The time spent by a target within a sensor's home area follows uniform random statistics. The home area of the sensor is the area guarded by it when it is stationed at its home position, its default position when it is not in pursuit of a target. The framework is further extended to situations where multiple sensors monitor the same home area. Simulation results presented corroborate with the probabilistic framework developed and verify its correctness for single as well as multi-sensor cases.

1. Introduction

Automated surveillance systems require observation of multiple targets from multiple locations with the possibility that monitoring sensors are mobile. There have been many approaches in the literature that deal with the problem of multi sensor based observation and tracking of multiple targets [1,4–12]. Based on their survey the authors have not come across formal methods of obtaining a desired system performance or methods that provide some form of guarantee or completeness for their performance. There are several ways of measuring the performance of a sensor network such as the number of targets detected, median number of detections, number of missed targets or energy measures. This paper presents a methodology for obtaining desired system performance such that a fraction of targets expected to crisscross the home area of a sensor will always be noticed within probabilistic guarantees by controlling the tracking time of the sensors.

The proposed approach is particularly suitable for guarding large open areas that are crisscrossed by moving targets and the number of sensors at disposal for monitoring them is limited. Due to limited number of sensors as well as to glean characteristics of targets over several observations the sensors are entailed to be mobile frequently. Such systems find utilities in many security, surveillance and reconnaissance applications.

The surveillance system is as shown in Fig. 1. Each sensor guards in its default stationary state an area called the home area of the sensor. For a sensor s_j, its home area is denoted by H_j. The sensors monitor a square surveillance zone. The surveillance zone is divided into number of square shaped cells as shown in Fig. 1 for the sake of modeling. The shaded circles are the sensors placed in their home positions. The radius of vision of the sensor equals the length of the diagonal of the cell. The field of vision (FOV) of the sensor is 360 degrees. However the sensor only considers those targets that lie within its four neighboring cells as targets within its field of vision to facilitate faster computations of certain statistical values. This simplification does not have any bearing on the overall philosophy

*Corresponding author.

ISSN 1069-2509/05/$17.00

of the approach. The area representing the FOV in its home position is called the home area of that sensor. The home area of each sensor is depicted by thick boundaries and encompasses four cells. The crosses just outside the surveillance zone are the source points from which targets emanate as per Poisson statistics.

A sensor allocates itself to one of the targets within its field of vision through a resource allocation process modeled through fuzzy rules [1]. The sensor further decides if it would monitor the target by remaining stationary or by pursuing (tracking) it. When a sensor tracks a target it leaves areas in its home position unguarded. The tracking time for a sensor s_j, denoted by t_j represents the time for which the target would be away from its home position H_j. The tracking time can be modulated based on the fraction of the number of targets that a sensor is expected to detect for a specified probabilistic guarantee. If $\hat{N}_T$ denote the number of targets expected to crisscross H_j within a temporal window Γ and f be the lower bound on the fraction of the number of targets, $\hat{N}_\Gamma$, to be detected and Ω represent the guarantee the paper presents a framework for computing $t_j = g\left(\Gamma, f, \hat{N}_T, \Omega\right)$. Here g is a function that ensures at least a fraction $f$of the expected targets, $\hat{N}_\Gamma$, are detected to a probabilistic guarantee Ω. In other words $g : P\left(n \geqslant f \cdot \hat{N}_\Gamma\right) \geqslant \Omega$, where P is the probability computation over the random variable n that denotes the number of targets detected.

The rest of the paper is organized as follows. Section 2 places the current work in the context of similar works found in the literature. Section 3 presents the formulation of the methodology and Section 4 depicts the efficacy of the methodology in simulations. Section 5 extends the formulation to an environment where multiple sensors are placed with the responsibility of guarding the same home area. Section 6 comments on the approximations used in the framework and Section 7 concludes and provides further scope of this work.

2. Background review

Many security, surveillance, and reconnaissance systems require distributed autonomous observation of movements of targets navigating in a bounded area of interest. Multi sensor surveillance finds applications such as in border patrol, guarding of secured areas, search and rescue and warehouse surveillance [15]. It involves detection of multiple intrusions and/or tracking through coordination between the sensors. Detection and target tracking has been researched from multiple viewpoints. Some efforts have focused on the problem of identifying targets from a given set of data through particle filters [2], and probabilistic methods [3]. The problem of data association or assigning sensor measurements to the corresponding targets were tackled by Joint Probabilistic Data Association Filters by the same researchers such as in [2]. Kluge and others [4] use dynamic timestamps for tracking multiple targets. Krishna and Kalra [5] presented clustering based approaches for target detection and further extended it to tracking and avoidance. The focus of these approaches has been on building reliable estimators and trackers. They do not use distributed sensors and are not directly useful for the problem of large area surveillance.

In the context of distributed task allocation and sensor coordination Parker [6] proposed a scheme for delegating and withdrawing robots to and from targets through the ALLIANCE architecture. The protocol for allocation was one based on “impatience” of the robot towards a target while the withdrawal was based on “acquiescence”. Jung and Sukhatme [7] present a strategy for tracking multiple intruders through a distributed mobile sensor network and present a strategy for maximizing sensor coverage in [8]. Lesser’s group have made significant advances to the area of distributed sensor networks [9] and sensor management [10]. In [7] robots are distributed across a region using density estimates in a manner that facilitates maximal tracking of targets in that region. The decision for a robot to move to another region or to stay in its current region is based on certain heuristics. In [11] Parker presents a scheme called A-CMOMMT where the goal is to maximize the number of targets observed over a time interval of length T based on the same philosophy of behavior-based control as in [6]. The paper however does not delineate a formal mechanism for maximizing target observations but compares four behavior based approaches. The authors of this paper present their scheme for resource allocation and coordination in a distributed sensor system through a set of fuzzy rules in [1] and further analyze the behavior of system by varying the autonomy of the sensors in [12].

In none of the above efforts is a strategy for guaranteeing some form of completeness is presented. Based on their survey the authors find this paper novel and different from other efforts in multi-sensor systems in that it offers a tracking strategy for sensors that modulates their tracking time such that a required number

of targets are detected within probabilistic guarantees. The authors in [13] present a framework that provides for meeting a targeted search time within probabilistic guarantees for a cooperated UAV search. The UAVs search a hostile environment for targets capable of firing them. A critical time is fixed by the user, which if exceeded the operation is deemed a failure. The framework computes the minimum number of UAVs required for a successful search operation within probabilistic guarantees. The basis of their framework contrasts with this in that the number of UAVs varies and the search time is fixed, whereas the number of sensors is fixed while the tracking time varies in this approach. Also the computations for their framework are disparate from this effort and are presented for a different application and motivation.

3. The methodology

Targets are modeled percolating in a Poisson fashion at the rate $\lambda$from the target sources shown in Fig. 1 into that horizontal or vertical half-plane that contains the surveillance zone. Therefore, all targets coming from a particular source will be contained within an angular span of πradians. Furthermore, the following assumptions are made for sensors and targets

1. A sensor can detect all targets within its FOV or occlusion relations are not considered.
2. The takeoff angle of a target from its source point is uniformly distributed in $[0, \pi]$
3. All targets move with the same uniform velocity within the surveillance zone along linear trajectories, which can be ascertained by the sensor.

The third assumption allows values such as $T_{esc,j}$ used in equation (2) to be evaluated with lesser computations. Otherwise such computations would require a probability distribution for the velocity of targets, which makes computations more intense. Assumptions 2 and 3 results in a piecewise uniform distribution $T_{esc,j}$ the computation of which is explained later.

The value of λ is 0.1 for all the examples discussed in this paper. Then the apparent rate at which each sensor, sj would see a target, λ_{sj} is given by $\lambda_{sj} = \lambda \sum_{k=1}^{P} \frac{\theta_k}{\pi}$, where, the ratio $\frac{\theta_k}{\pi}$ denotes the expected fraction of the total number of targets that would enter the home area of s_j from the kth of the P target source points. For Fig. 1 there are 24 source points represented by crosses. We also denote by $\lambda_{sj,k} = \lambda\frac{\theta_k}{\pi}$ the rate at which sj sees targets from source k. In other words, among the targets taking off at any angle within $[0, \pi]$, from source k only those that takeoff within the angular span $[\delta_k, \delta_k + \theta_k]$ would enter the FOV of the sensor, where δ_k is the smallest angle formed by the segment connecting a vertex of the FOV square of sj and source k and $\delta_k + \theta_k$ is the largest angle. Let n be the random variable denoting the number of detections made over a temporal window Γ. The probability of detecting exactly k of the N_Γ targets expected to arrive in Γ by a sensor sj within its home area H_j is given by the familiar binomial distribution $P\left(n = k \middle/ X = \hat{N}_\Gamma\right) = \binom{\hat{N}_\Gamma}{k} p^k (1-p)^{\hat{N}_\Gamma - k}$. Here X is a Poisson random variable that measures the number of arriving targets and p represents the probability that a target would be detected by the sensor. The resultant probability of detecting k such targets then becomes $P(n = k) = P\left(n = k \middle/ X = \hat{N}_\Gamma\right) \cdot P\left(X = \hat{N}_\Gamma\right)$. It can be shown that the above resultant probability once again has a poisson distribution with parameter $\lambda_{sj}p$. Hence the probability of detecting k targets has the representation

$$P(n = k) = e^{-\lambda_{sj}p} \frac{(\lambda_{sj}p)^k}{k!} \tag{1}$$

We now fix the binomial probability of detection of a target by a sensor within its home area empirically as

$$p = \frac{T_{esc,j}}{T_a} \tag{2}$$

Here $T_{esc,j}$ is the expected time for which a target is likely to be inside the home area of sj, the computation of which is briefed later and T_a is the apparent time for which the target perceives the sensor to be away. The apparent time highlights that a sensor while moving away from its home position continues to observe a part of the home area for some time before leaving its home area completely unguarded. Till such time the area is left completely unguarded, the time for which the sensor is away is reduced by a factor T_κ within the integral shown below

$$T_a = \begin{cases} 2\int_0^{t_j/2} \frac{t}{T_K} dt; & t_j \leqslant 2T_\kappa \\ 2\int_0^{T_\kappa} \frac{t}{T_\kappa} dt + 2\left(t - T_\kappa\right)_{T_\kappa}^{t_j}; & t_j > 2T_\kappa \end{cases} \tag{3}$$

In (3) t_j is the actual time sensor sj is away from its home position, its tracking time. t/T_κ represents the fraction of the area left unguarded after t samples from

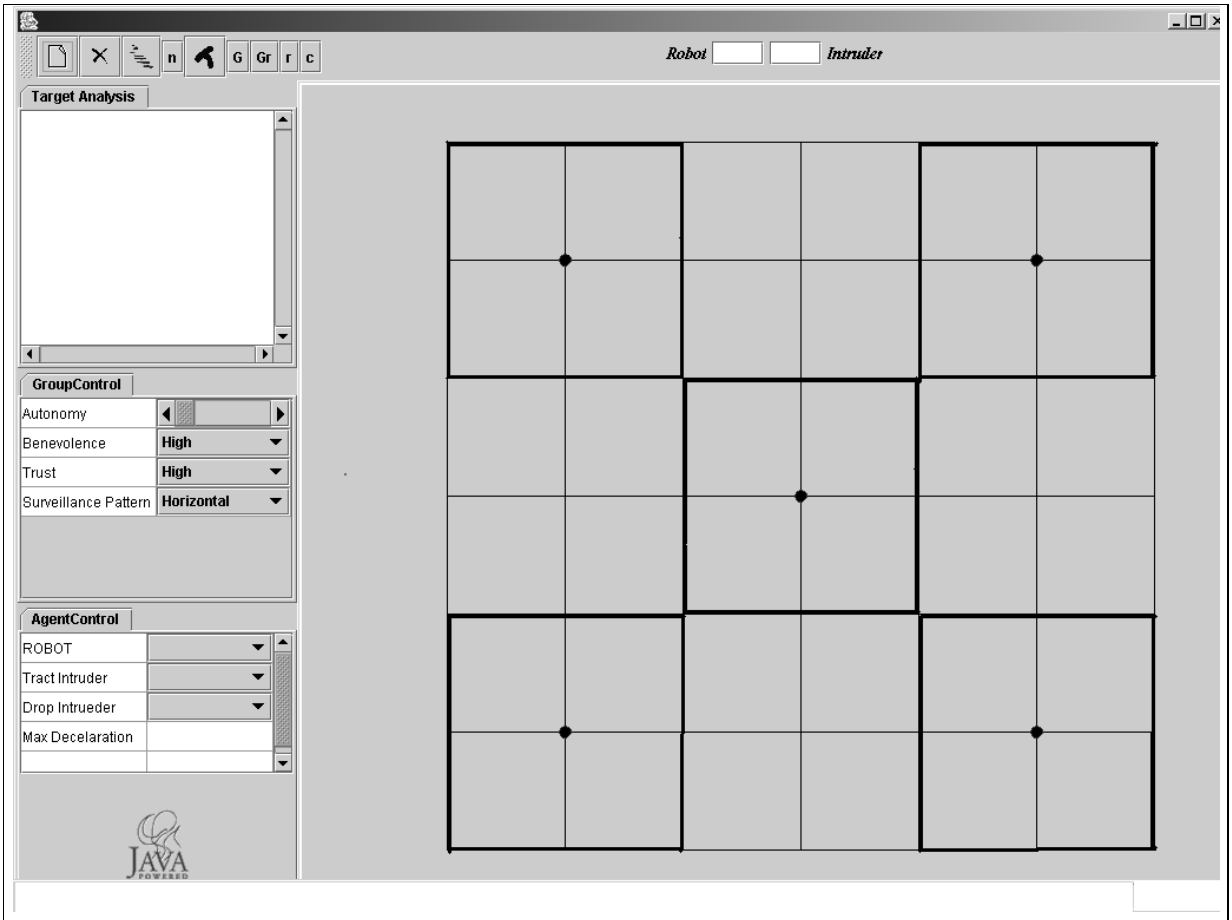

Fig. 1. The rectangular surveillance zone with sensors depicted as circles ensconced in their home positions. The home area of each sensor is denoted by thick squares.

the tracking onset. The upper limit of the integral T_κ denotes the time at which the sensor leaves its original area completely unguarded.

The tracking time t_j is eventually computed by making use of Eqs (1), (2) and (3) and that which would satisfy the following guarantee condition:

$$P\left(n = k \geqslant f \cdot \hat{N}_t\right) \geqslant \Omega \tag{4}$$

The numerator of Eq. (2) depicts the expected time a target would stay within the home area of a sensor assuming Poisson statistics of entry and uniform random statistics for time of stay within the sensor's home area. Similarly the denominator of (2) suggests the likely time for which the target perceives the sensor to be away while the sensor itself is in motion. While the numerator is a constant for given target statistics and home area geometry, the denominator would vary based on current location of the sensor such as if it is inside or outside its home area and its motion direction (if it is going away from its default location of coming towards it). The philosophy behind Eq. (2) can be construed in the following way. The binomial probability of detection should be higher if the expected time before which the target escapes from the home area is high or if the apparent time the target perceives the sensor to be away from the surveillance zone is low. In other words if the target spends longer durations within its home area or if the sensor does not go too far away from its home position the probability of a sensor detecting a target increases and vice versa. Equation (2) tries to capture this reasoning by placing the concerned terms in the numerator and denominator.

The formulation is described graphically through Figs 2(a) and 2(b). Consider a sensor into whose home area targets are expected to enter at a rate $\lambda_{sj} = 0.5$. Then over a time interval of 20 units the expected number of arrivals is either 9 or 10. This is shown in Fig. 3(a) with the mean expected arrival showing a peak in the

probability distribution function at 9 and 10. If a fraction of at least $f = 0.7$ of these targets (7 of them) are to be detected with a minimum guarantee of $\Omega = 0.55$ the rate at which the sensor detects, $\lambda_{SJD} = \lambda_{SJ}p$, is computed to be 0.4 and the binomial detection probability of a target turns out as $p = 0.8$. Having computed p the wandering time of the sensor t_j is derived from Eqs (2) and (3). The dotted vertical line in Fig. 2(a) indicates the lower bound on the fraction of the number of arriving targets that needs to be detected using the above guarantee. The only constraint on the user in fixing the guarantee is that $\lambda_{sjd} \leqslant \lambda_{sj}$ needs to be obeyed. In other words the rate of detection cannot be greater than the rate of arrival.

The expected time a target from source i is likely to be within the home area of sj before it escapes, $T^i_{esc,j}$, is modeled through uniform random statistics. Depending on the points of entry into and exit from the home area, some portions between the lower and upper bound of the distribution $[t_l, t_u]$ could be more frequent than the others. Hence the normalization constant for the distribution is not uniform throughout. These details are taken care while computing the normalization constant of the uniform distribution for every target source. Thus $T^i_{esc,j}$ the expected time a target coming from source i would last in the home area of sj is given by

$$T^i_{esc,j} = \int_{t_l}^{t_{l+1}} \eta_1 t dt + \int_{t_{l+1}}^{t_{l+2}} \eta_2 t dt + \ldots + \int_{t_{l+u-1}}^{t_u} \eta_u t dt, \tag{5}$$

Here $\eta_1, \eta_2, \ldots, \eta_u$ are constants of proportionality corresponding to various portions such that

$$\int_{t_l}^{t_{l+1}} \eta_1 dt + \int_{t_{l+1}}^{t_{l+2}} \eta_2 dt + \ldots + \int_{t_{l+u-1}}^{t_u} \eta_u dt = 1 \tag{6}$$

Omitted here for brevity the methodology that describes the computation of $\eta_1, \eta_2, \ldots, \eta_u$ and their corresponding intervals $[t_l, t_{l+1}], \ldots, [t_{l+u-1}, t_u]$. The overall expected escape time for a target within the home area of any sj is then given by $T_{esc,j} = \frac{\sum_{i=1}^{P} \lambda_{sj,i} T^i_{esc,j}}{\sum_i \lambda_{sj,i}}$, the weighted average over the expected time corresponding to various sources.

Since double precision arithmetic does not allow computation of factorials beyond 20 the normal approximation to poisson distribution is used in our computations.

4. Simulation results

The first objective is to evaluate empirically the validity of Eq. (2) that ascertains the probability of detecting a target by a sensor while it is in motion. For this purpose a single cell environment with one sensor such as in Fig. 3 is considered. Targets are introduced in poisson fashion at the midpoints of the four boundaries of the cell. The sensor's home position is at the center of the cell. The wandering time t_j is calculated for a given value of Ω and f. The sensor is away from its home position for t_j units. The sensor does not resource allocate and track a particular target. It is merely away from its home position. The number of targets that crisscrossed the cell during this time interval and the number of those detected were recorded.

The results are tabulated in Table 1. The first column represents the desired fraction of the targets that need to be detected and the second the minimum probabilistic guarantee of detecting the fraction. The third column is the actual fraction of the targets detected averaged over twenty runs. The fourth column signifies the relative frequency of times a fraction greater than or equal to the desired fraction was detected. The fourth column is then a means of evaluating whether the desired probabilistic guarantee was obtained. If the desired fraction to be obtained is 0.8 with guarantee 0.6 and thirteen times out of twenty a fraction more than 0.8 was detected, the entry in the last column of the table is $13/20 = 0.65$ that signifies the required performance was met. It is seen that the average obtained fraction is above the desired fraction whenever the minimum probabilistic guarantee is high indicating that the desired fraction was detected in most of the runs as entailed by the guarantee. The average fraction obtained is lesser than the desired fraction when the desired probabilistic guarantee is low. This is indeed expected as a low desired guarantee indicates that the sensor is entailed to detect the desired fraction of targets only in a few of those twenty runs. The relative frequencies in the fourth column also do not fall significantly below the desired minimum probabilistic guarantee in any of the runs. That the relative frequency is within 5–10% of the desired guarantee in all the runs validates the

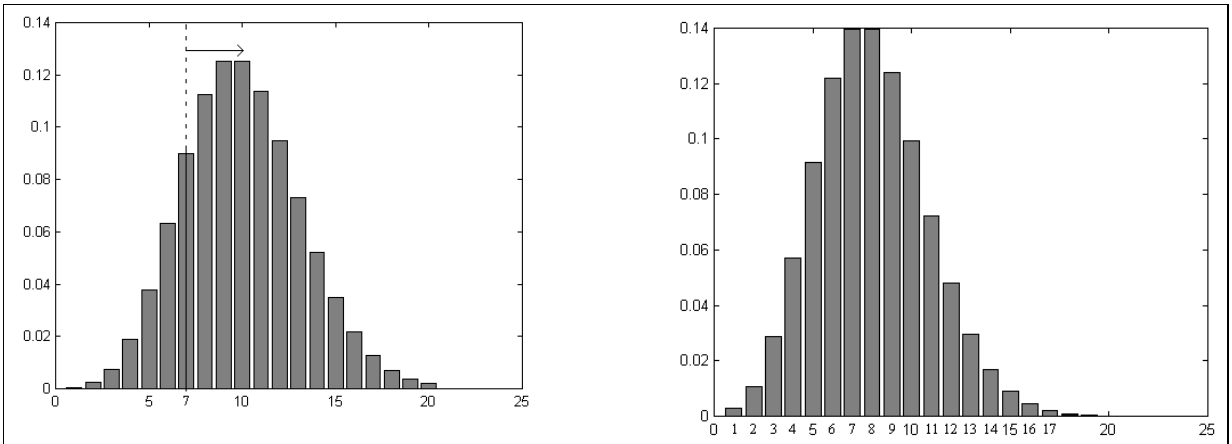

Fig. 2. (a) The probability distribution function for target arrivals. The mean expected number of target arrivals over an interval of 20 units is 10. The dotted line and the arrow to the right indicates a minimum of 7 targets need to be detected by the sensor. (b) The probability distribution function for target detections for a minimum guarantee of 0.55 for the arrival distribution shown in Fig. 2(a). The mean expected number of detections is 7.

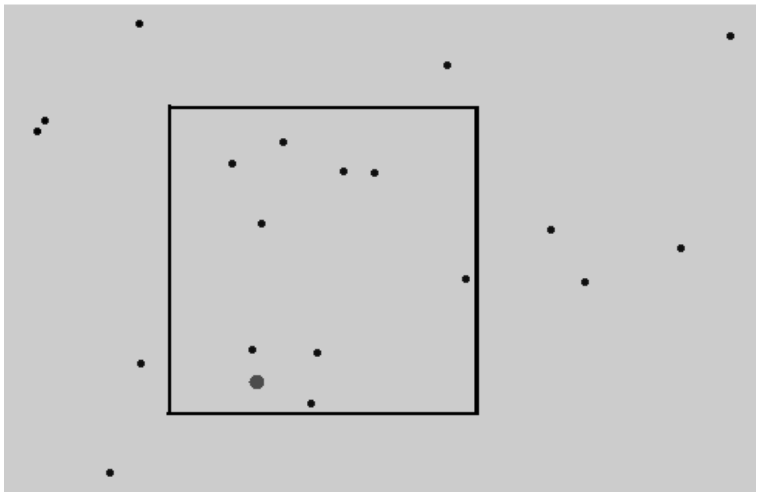

Fig. 3. A single cell environment used for validating the definitions of Eqs (2) and (1). The bigger circle denotes the sensor and the smaller circles the crisscrossing targets introduced in poisson fashion.

probability definition of Eq. (2) and the computation of apparent time in Eq. (3).

The framework developed in Section 3 is now tested for an environment shown in Fig. 1 with multiple sensors. Each sensor tracks targets such that the probabilistic guarantee is maintained with respect to its home area. The overall quality of track (*QoT*) at the end of a simulation interval Γ is defined by:

$$QoT = \frac{1}{N_S} \sum_{j=1}^{N_S} \frac{n_{dj}}{n_{cj}} \quad (7)$$

In Eq. (7) N_S denotes the total number of sensors in the environment, n_{dj} denotes the number of targets detected by the sensor among those that had visited its home area H_j, while n_{cj} is the number of targets that had been through H_j. Thus $\frac{n_d}{n_c}$ represents the fraction of the targets that entered a sensor's H_j and were detected by it. Thus Eq. (7) represents the average fraction of targets detected over the simulation interval by the sensor network.

In the simulations that follow a sensor leaves its environment in pursuit of a target. Sensors can reallocate themselves to other targets during the course of a track

Table 1
Tabulation of the results obtained for the environment of Fig. 3 for different desired fraction and guarantee values

Desired minimum fraction (f)	Desired minimum probabilistic guarantee (Ω)	Obtained average fraction (20 runs)	Obtained relative frequency (20 runs)
0.9	0.9	0.91	0.95
0.9	0.1	0.23	0.05
0.6	0.9	0.73	0.85
0.6	0.1	0.38	0.2
0.4	0.6	0.42	0.65
0.4	0.4	0.32	0.3
0.1	0.9	0.28	1
0.1	0.1	0.08	0.2

as dictated by the resource allocation strategy [1]. The time t_j for a sensor is updated after every fixed number of samples based on the fraction of the targets that were detected thus far, f_d, and the fraction that need to be detected in the remaining time window, f_r, to meet the objective of Eq. (4). Both f_r and f_d can take values greater than 1. Fraction f_r goes above 1 when the sensor is away sufficiently long from its home position and the number of targets it needs to detect in the remaining time in order to have detected the desired fraction f is greater than the number expected to arrive. Fraction f_d is the number of targets detected thus far divided by the expected number of arrivals at H_j thus far. If targets arrive at a rate faster than the expected arrival rates for a portion of simulation interval f_d can be above 1 for those intervals.

Figure 4 shows a snapshot of a simulation run. The bigger circles represent the sensors and the smaller circles the targets. The dashed rectangles enclosing the sensor and target identify the sensor-target pair (the target to which the sensor has allocated itself to). It is to be noted while a sensor tracks a target it also detects all other targets within its field of vision due to assumptions stated before. The problems of data association are also not considered. As a consequence the number of detections by a sensor at any instant is all those within its FOV.

4.1. Analysis

Figure 5(a) shows two graphs that plot f_r, the fraction remaining and wander time, t_j, along the y-axis. In both the graphs the abscissa denotes the time in samples. Sampling measurements on f_r, t_j are done once in every ten cycles of a simulation run. The total number of simulation cycles is 150 or in other words $\Gamma = 150$ in these simulations. Each cycle is repeated every 500 ms. The graphs cover the entire simulation run of 150 cycles or 15 samples of measurements. The plot of Fig. 5(b) depicts QoT on y-axis and sample time on x. Both graphs 4a and 4b are for a simulation run with parameter $f = 0.8,\ \Omega = 0.75$. The graphs of Fig. 5(a) are for one of the sensors of Fig. 3 while graph 5b depicts QoT of the entire system. Graphs in Figs 5(c) and 5(d) have the same connotations as in Figs 5(a) and 5(b) except that they are for parameters $f = 0.8,\ \Omega = 0.3$. The horizontal dashed line in the graph of 5b and 5d indicate the desired fraction of target fraction of targets, f, expected to be detected at the end of the simulation. Since QoT as defined in Eq. (7) computes the fraction of targets detected averaged across all the sensors in the system, the horizontal line serves as an indicator if the QoT was achieved or not.

For $\Omega = 0.75$ the track time is modulated such that the desired fraction $f$averaged over all sensors is detected at the end of a simulation run for majority of such runs. Figure 5(b) corresponds to one such run where the track quality at the end of the simulation is 0.85 and is above the expected criterion of 0.8 and lies above the horizontal. Figure 5(d) corresponds where the QoT at the end of the simulation does not achieve the desired fraction. This is expected for a run with $\Omega = 0.3$ where most of the runs are not required to detect a fraction greater than 0.8.

For a marginal increase in f_r in the top plot of Fig. 5(a) the corresponding decrease in t_j is steeper in the bottom plot of 5a when compared with Fig. 5(c). The decrease in wander time t_j as f_r increases is less steep in 5c than in Fig. 5(a). For a given f the variations in t_j are due to the variations in Ω. A higher Ω entails that the sensor cannot move too far away from its home due to lower values of t_j. As the sensor moves away from its home and misses targets the required remaining fraction to be detected f_r may tend to increase. In such a case the decrease in wander time also tends to be steeper for a similar increase in f_r for a higher Ω. A steeper increase translates as quicker returns to home by the sensor to detect more targets.

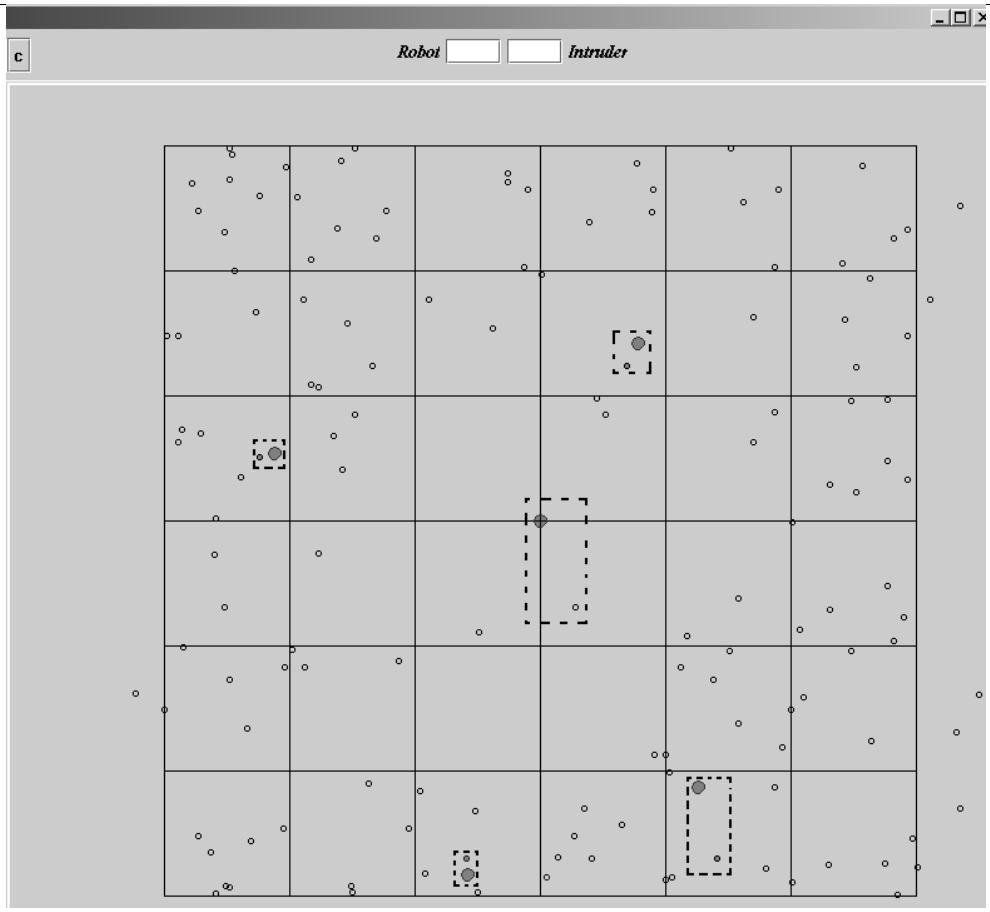

Fig. 4. A snapshot of a simulation run. The dotted rectangles enclosing a sensor-target pair indicate the target to which that sensor is currently allocated to. Sensors are shown by larger circles while targets are depicted smaller.

5. Extension to multi sensors

The framework is now extended for the case when multiple sensors guard the same home area. Intuitively it is expected that, when P in Eq. (4) represents the joint probability of a system of sensors the corresponding individual binomial probabilities would be lower and hence the wander time for a sensor would be higher. In Fig. 6 each home area, whose boundaries are depicted thick are guarded by two or three sensors, one placed at the center and the remaining at the corners. Let s_{j0} denote the center sensor of H_j and $s_{j1},\ s_{j2}$ its corner sensors. A corner sensor would itself be a center sensor for another home area H_i. Let the overall binomial probability of detection that satisfies the guarantee Eq. (4) for H_j be p_j. In the generalized case of n sensors guarding H_j with their individual binomial probabilities being $p_{j1},\ p_{j2},\ \ldots, p_{jn}$ we have

$$p_j = p_{j1} \cup p_{j2} \cup \ldots \cup p_{jn}. \quad (8)$$

To find the individual p_{ji} of each sensor that satisfies the overall p_j results in a search in the space of probabilities that even after discretization is very large, exponential in the number of sensors. It is large for more than two sensors. Instead we seek a closed form solution for Eq. (3) by first computing the expected value of T_κ as $\hat{T}_\kappa$, the time at which the sensor leaves the area unguarded. It is to be noted that T_κ used in Eq. (3) can only be computed on the fly, while the sensors are in motion based on their current motion direction and the time for which they have been already away from their home position. On the other hand, $\hat{T}_\kappa$, enables to know apriori the average value or the most likely value of T_κ. This is especially so if the number of reallocations to targets during a sensor sojourn is minimized. Under zero reallocation during sensor motion $\hat{T}_\kappa$ gives the true estimate of the expected time at which a sensor is likely to leave a home area completely unguarded. Since reallocation during motion makes sensor trajec-

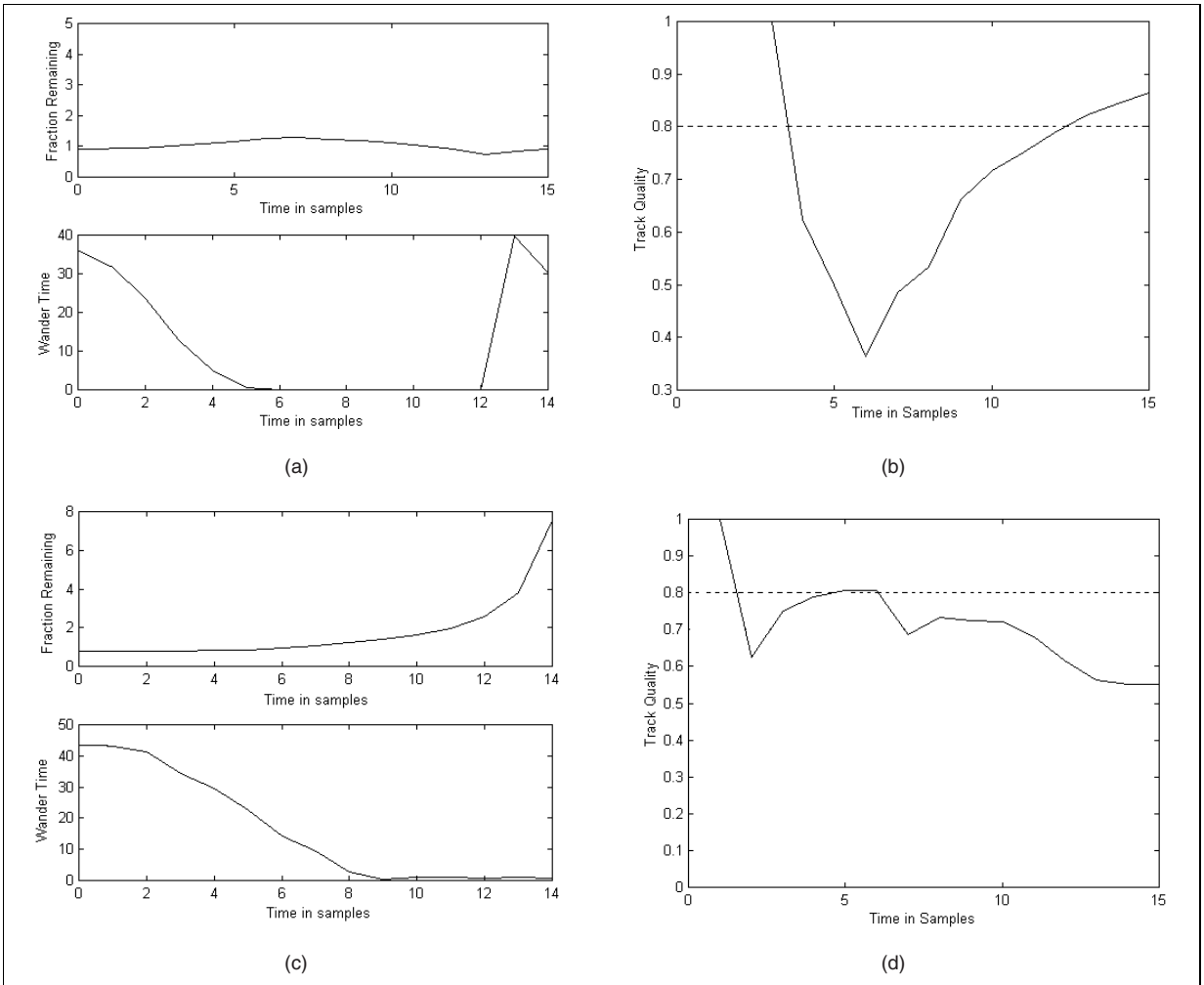

Fig. 5. (a) The top graph shows f_r plotted against sample time while the bottom graph is a plot of t_j against samples. The plots are for a simulation such as in Fig. 5 run with $f = 0.8,\ \Omega = 0.75$; (b) A plot of track quality QoT. The dashed horizontal line denotes the desired fraction of the total targets that need to be detected; (c) Graph same as Fig. 5(a) for parameters $f = 0.8, \Omega = 0.3$; (d) Graph with same connotations as Fig. 5(b) for parameters $f = 0.8, \Omega = 0.3$. At the end of simulation time the track quality is below the horizontal line indicating that performance criterion was not met.

tories piecewise linear the estimates of $\hat{T}_\kappa$ are always conservative in that the sensors are most likely to spend longer time within the home area due to piecewise linear motion than a purely linear motion. In other words when $\hat{T}_\kappa$ is used instead of T_κ in Eq. (3) the corresponding binomial probability in Eq. (2) can only be higher and the wander time of the sensor can only be lower. The computation of $\hat{T}_\kappa$ is along lines similar to the computation of T_{esc} making use of uniform random statistical distribution that governs the stay of a target within the home area of a sensor. The details of which are not discussed here to preserve brevity.

Once $\hat{T}_\kappa$ is computed a closed form analytic solution for Eq. (8) becomes possible by exploiting the fact that each of the p_{ji} has a form similar to Eq. (2). Hence we can denote $p_{ji} = \alpha_{j1} p_{j1}$ that results in a polynomial of order n. For two sensors guarding H_j the quadratic is easily solved and for three sensors the cubic is solved by Cardano's method [14].

For a system such as in Fig. 6 a sensor then has two or three individual binomial probabilities corresponding to the respective home areas it guards. Currently the algorithm adopts a conservative approach by choosing the highest of those detection probabilities or correspondingly the minimum of the tracking times.

Based on apriori estimates of $\hat{T}_\kappa$ we compare the performance of a multi-sensor surveillance of a home area vis-à-vis single sensor surveillance through the graphs

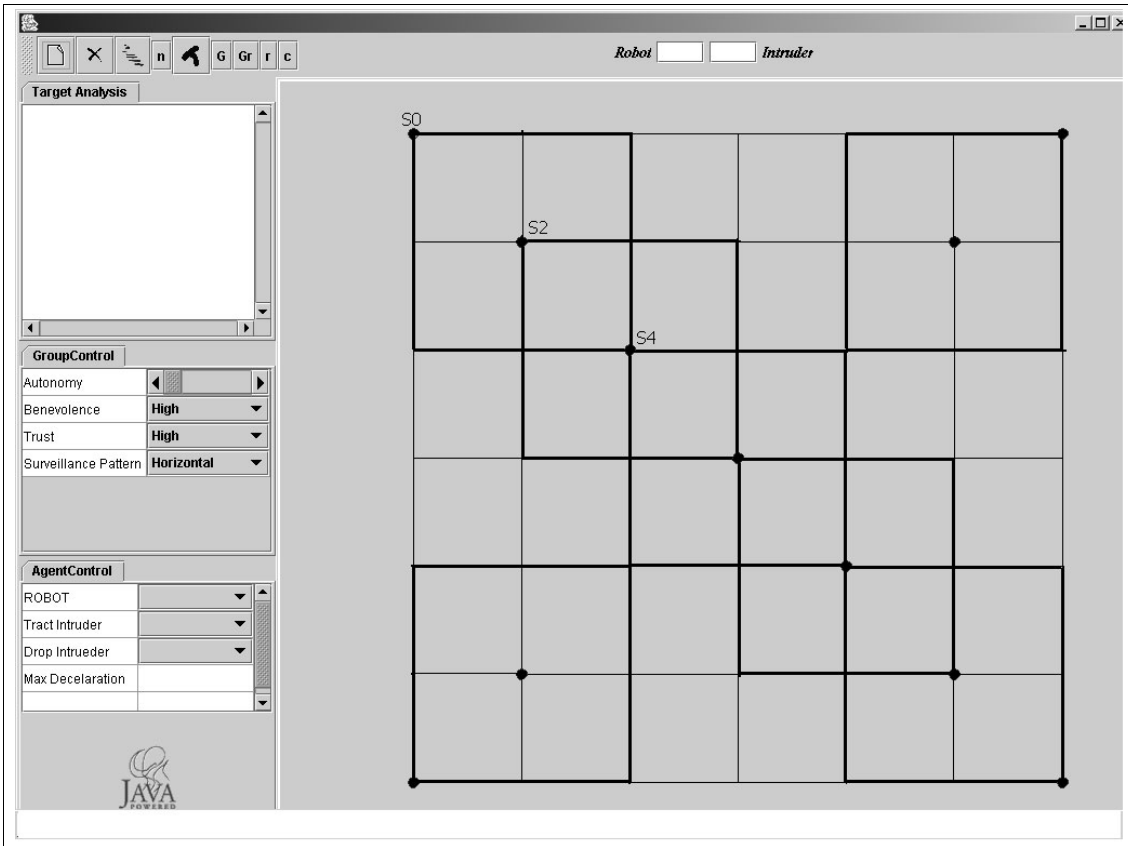

Fig. 6. A surveillance system in which each home area is guarded by more than one sensor (two or three).

of Fig. 7. The top graph of 7 depicts the individual probability of a sensor detecting a target for a fixed Ω (here 0.9) and varying f. The lower graph plots t_j versus f for a constant Ω (here 0.9). Each of these graphs shows three plots each. The plot with a dashed line corresponds to the case where a single sensor guards an area. The lower and upper solid lines in the top graph correspond to scenarios where three and two sensors guard the same area. The upper and lower solid lines in the lower graph corresponds to the wandering time for a triple sensor and double sensor scenario. The graphs confirm our intuition that the individual binomial probability decreases for every sensor added and the corresponding wander time increases. Since addition of more than three sensors results in solving difficult quartic, quintic and higher order polynomials the analysis is limited to a maximum of three sensors guarding the same home terrain.

The graphs of Fig. 7 predict the consequences of increasing the number of sensors with regard to individual binomial probability and wander time. The actual system performance is verified through simulations and their results depicted in Figs 8 and 9. The simulations reported are for the second sensor (S2) from the top left corner of Fig. 6 along the diagonal that connects the top left vertex to the bottom right of the surveillance zone. The home area for this sensor, S2, is also guarded by sensors S0 and S4, which are the corner sensors.

Figures 8(a) and 8(b) correspond to a simulation run for parameters $\Omega = 0.9, f = 0.8$. Figure 8(a) plots the fraction of targets detected so far, f_d, and binomial probabilities for triple and single sensor cases on the ordinate. The abscissa denotes the time samples at which these quantities where computed during a simulation run. The plot for a single sensor case in these figures is merely a reference and is represented by the dashed plot. The solid plot corresponds to the actual simulation scenario of three sensors guarding the home area of S2. The dotted line represents the fraction of targets detected so far. Figure 8(b) plots the wander time for the triple and single sensor cases (solid line and dashed line respectively) for the corresponding time samples

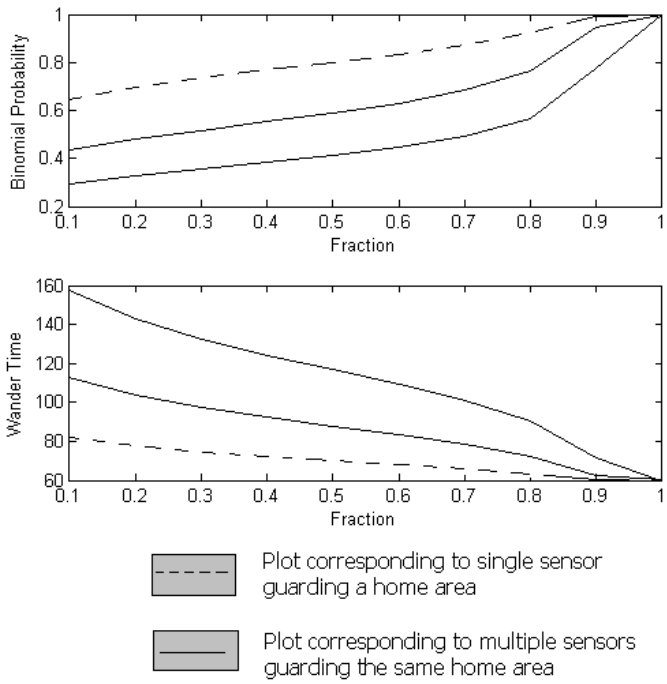

Fig. 7. Plots of individual probability and wander time against varying values of desired fraction f. Solid lines are plots corresponding to multiple sensors while dashed lines correspond to single sensor case. The lower and upper solid lines in the top graph and the upper and lower solid lines in the bottom graph correspond to scenarios where three and two sensors guard the same home area.

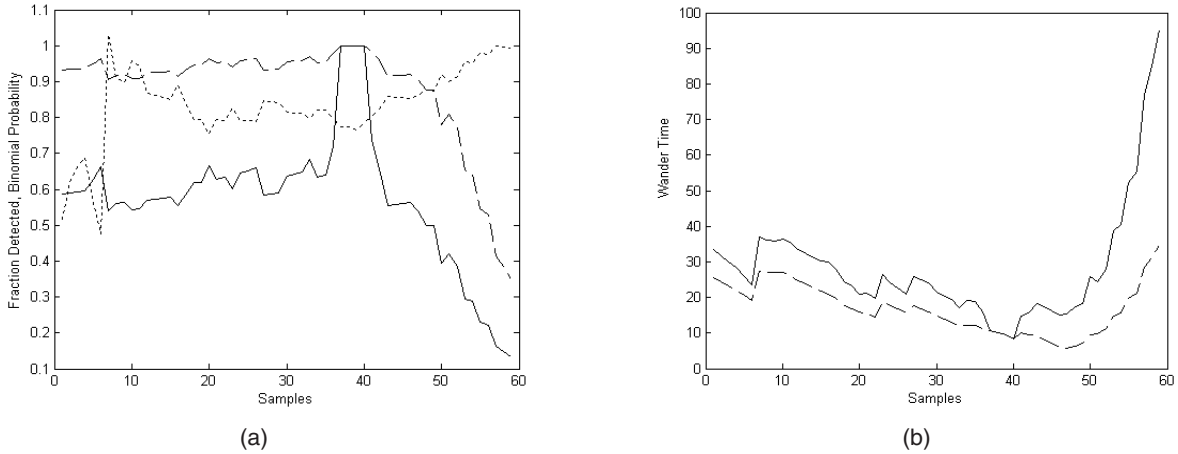

Fig. 8. (a) Plots of fraction of targets detected (dotted lines) so far and binomial probabilities for triple and single sensor (solid and dashed lines) cases on the ordinate. The abscissa denotes the time samples at which these quantities where computed. The plots are for $f = 0.8,\ \Omega = 0.9$; (b) Plots of wander time for triple sensor (solid line) and single sensor (dashed line) for the corresponding binomial probabilities at those time samples plotted in Fig. 8(a).

of simulations in Fig. 8(a). The plots obtained from actual simulations in 8 are similar to 7 in that the individual probabilities are lower and hence the corresponding wander times higher for the multi sensor case. Figure 8(a) confirms that the overall tracking performance was met for the multi-sensor scenario in that the fraction of targets detected at the end of the simulation was more than the required 0.8.

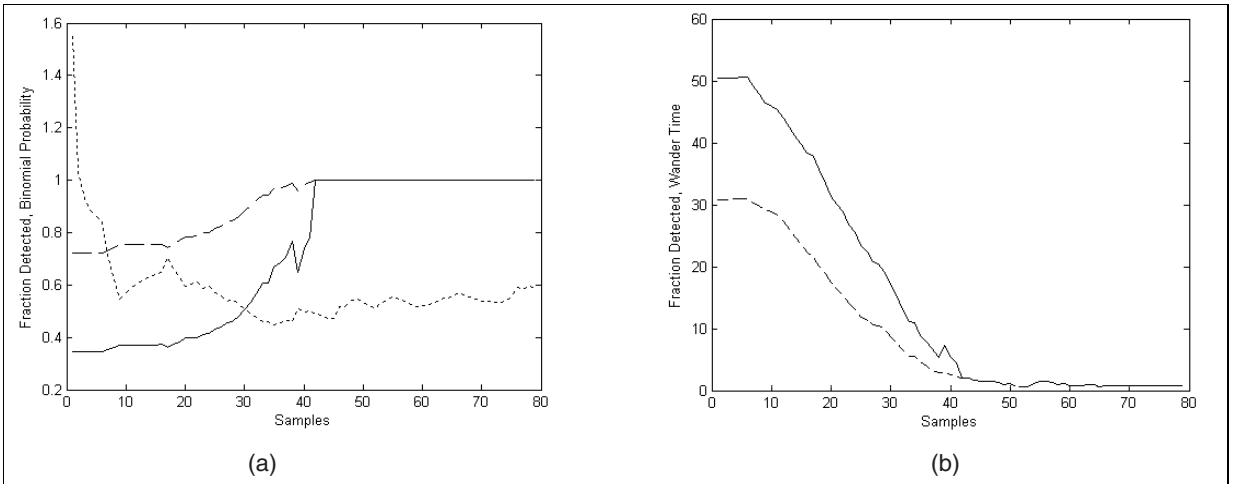

Fig. 9. (a) Graph same as Fig. 8(a) but for parameters $f = 0.8, \Omega = 0.2$ except that at the end of the simulation the fraction of targets detected is less than 0.8, close to 0.6 but this is due to the low probabilistic guarantee of 0.2; (b). Graph with same connotations as Fig. 8(b) for parameters $f = 0.8, \Omega = 0.2$.

Figures 9(a) and 9(b) are similar to those of 8a and 8b except that $\Omega = 0.2, f = 0.8$ for these simulations. Here the tracking performance is not met but that is agreeable considering the low probabilistic guarantee of 0.2. In this aspect the multi sensor simulations follow the single sensor simulations reported in Section 4 with regard to tracking performance being generally met for high Ω and not being met for low Ω. The binomial probability of individual sensors rises to 1 as the overall probability becomes 1 and the corresponding wander time falls to 0. Hence when the overall probability becomes 1 the individual probabilities and wander times for the single and multi-sensors converge to same values.

6. Closing comments

The framework presented in this paper is conservative in that the binomial probability of detection computed is generally more than the required amount and the wander time correspondingly lesser. This is due to the following approximations used in modeling.

The FOV used is the inscribed square of the actual circular FOV and hence the sensor always records lesser number of detections than it actually sees.

Multiple sensor cases are considered only when in their default home positions they share a part of the home area of another sensor. However during motion a sensor other than the center and corner sensors for that home area can enter the area and observe targets.

Due to process of reallocation sensors tend to spend longer time within the home area than due to purely linear motions.

Future frameworks would be directed to make the model more precise and less conservative by reducing some of these approximations.

7. Conclusions and scope

While there has been intense activity in software simulation of multi-sensor systems for surveillance there have not been many formal methods that provide for some form of guarantee or completeness in their performance. This paper has presented a framework that provides for probabilistic guarantees for a multi-sensor based multi-target tracking system. Sensors modulate their tracking time such that a desired fraction of targets would be detected to an arbitrary probabilistic guarantee. Hence the approach limits the upper bound of fraction of targets that can go undetected to any subjective probabilistic accuracy. As a consequence the method also defines a yardstick for measuring detection performance – based on the fraction of targets detected under the constraint of sensor mobility and target pursuit that leaves areas unguarded through which other targets can escape unnoticed. The proposed approach is particularly suitable for guarding large open areas that are crisscrossed by moving targets and the number of sensors at disposal for monitoring them is limited. Due to limited number of sensors as well as to glean characteristics of targets over several observations the

sensors are entailed to be mobile frequently. Such systems find utilities in many security, surveillance and reconnaissance applications.

Extension of the scheme to multiple sensors guarding the same area enables longer tracking time for a sensor due to lower binomial probabilities for the same guarantee. Increased wandering time can lead to better tracking performance in terms of median and mean number of tracks as reported in [2]. Simulation results presented corroborate with the probabilistic framework developed and vindicate its correctness for single as well as multi-sensor cases.

The future scope of this work is multifarious where the authors expect to develop following frameworks:

Multi-sensor coordination of optimal tracking of targets in the sense of maximizing target detections T time samples into the future

Multi-sensor coordination for repeatable probabilistic guarantees for the entire surveillance zone: While the current effort deals with guaranteeing completeness for the home area of the sensor, a logical extension would be to develop models for coordination that results in sensors modifying their allocation and tracking time such that a completeness with respect to entire surveillance zone is achieved.

Multi-sensor coordination for a combination of various optimal guarantees where we propose to come up with models that provide for a combination of various performance measures such as a combination of 1 and 2.

References

[1] K.M. Krishna, H. Hexmoor and S. Pasupuleti, A Surveillance System Based on Multiple Mobile Sensors, *Proceedings of FLAIRS* (2004), Special Track in Sensor Fusion.

[2] D. Schulz, W. Burgard, D. Fox and A. Cremers, Tracking multiple moving targets with a mobile robot using particle filters and statistical data association, *IEEE International Conference on Robotics and Automation* (2001), 1165–1170.

[3] D. Schulz and W. Burgard, Probabilistic state estimation of dynamic objects with a moving mobile robot, *Robotics and Autonomous Systems* (2001).

[4] B. Kluge, C. Kohler and E. Prassler, Fast and robust tracking of multiple objects through a laser range finder, *IEEE International Conference on Robotics and Automation* (2001), 1165–1170.

[5] K.M. Krishna and P.K. Kalra, Detection tracking and avoidance of multiple dynamic objects, *Journal of Intelligent and Robotic Systems* **33**(4) (2002), 371–408.

[6] L. Parker, Cooperative robotics for multi-target observation, *Intelligent Automation and Soft Computing* **5**(1) (1999), 5–19.

[7] B. Jung and G.S. Sukhatme, *Multi-Target Tracking using a Mobile Sensor Network*, Proc., IEEE Intl. Conf. On Robotics and Automation, 2002.

[8] S. Poduri and G.S. Sukhatme, Constrained Coverage for mobile sensor networks, *IEEE ICRA* (2004), 165–171.

[9] L. Parker, Distributed algorithms for multi-robot observation of multiple moving targets, *Autonomous Robots* **12**(3) (2002).

[10] B. Horling, R. Vincent, R. Miller, J. Shen, R. Becker, K. Rawlins and V. Lesser, *Distributed Sensor Network for Real Time Tracking*, in Proceedings of the 5th International Conference on Autonomous Agents, 2001, 417–424.

[11] B. Horling, R. Miller, M. Sims and V. Lesser, *Using and Maintaining Organization in a Large-Scale Distributed Sensor Network*, in Proceedings of the Workshop on Autonomy, Delegation, and Control, (AAMAS 2003).

[12] K.M. Krishna, H. Hexmoor and S. Pasupuleti, Role of Autonomy in a Distributed Sensor Network, *Proceedings of ICAI* (2004).

[13] P. Vincent and I. Rubin, A Framework and Analysis for Cooperative Search Using UAV Swarms, *Proceedings of SAC'04* (March 14–17), Nicosia, Cyprus.

[14] http://www.mathwright.com/library/oldcardanoxb.html.

[15] H.R. Everett, G.A. Gilbraeth and R.T. Laird, Coordinated control of multiple security robots, *Proceedings of SPIE Mobile Robots* (1993), 292–305.